



Contents lists available at ScienceDirect

## Bioorganic &amp; Medicinal Chemistry

journal homepage: [www.elsevier.com/locate/bmc](http://www.elsevier.com/locate/bmc)

# Novel, potent, orally bioavailable and selective mycobacterial ATP synthase inhibitors that demonstrated activity against both replicating and non-replicating *M. tuberculosis* ☆

Supriya Singh<sup>a</sup>, Kuldeep K. Roy<sup>a</sup>, Shaheb R. Khan<sup>b</sup>, Vivek Kr. Kashyap<sup>b</sup>, Abhisheak Sharma<sup>d</sup>, Swati Jaiswal<sup>d</sup>, Sandeep K. Sharma<sup>b</sup>, Manju Yasoda Krishnan<sup>b</sup>, Vineeta Chaturvedi<sup>c</sup>, Jawahar Lal<sup>d</sup>, Sudhir Sinha<sup>c</sup>, Arnab D. Gupta<sup>b</sup>, Ranjana Srivastava<sup>b</sup>, Anil K. Saxena<sup>a,\*</sup>

<sup>a</sup> Division of Medicinal and Process Chemistry, CSIR-Central Drug Research Institute, B.S. 10/1, Sector 10, Jankipuram Extension, Sitapur Road, Lucknow 226031, India

<sup>b</sup> Microbiology Division, CSIR-Central Drug Research Institute, B.S. 10/1, Sector 10, Jankipuram Extension, Sitapur Road, Lucknow 226031, India

<sup>c</sup> Division of Drug Target Discovery and Development, CSIR-Central Drug Research Institute, B.S. 10/1, Sector 10, Jankipuram Extension, Sitapur Road, Lucknow 226031, India

<sup>d</sup> Pharmacokinetics and Metabolism Division, CSIR-Central Drug Research Institute, B.S. 10/1, Sector 10, Jankipuram Extension, Sitapur Road, Lucknow 226031, India

## ARTICLE INFO

## Article history:

Received 8 September 2014

Revised 24 December 2014

Accepted 26 December 2014

Available online xxxxx

## Keywords:

Tuberculosis

ATP synthase

Quinoline

Sulfonamide

Dormancy

## ABSTRACT

The mycobacterial F<sub>0</sub>F<sub>1</sub>-ATP synthase (ATPase) is a validated target for the development of tuberculosis (TB) therapeutics. Therefore, a series of eighteen novel compounds has been designed, synthesized and evaluated against *Mycobacterium smegmatis* ATPase. The observed ATPase inhibitory activities (IC<sub>50</sub>) of these compounds range between 0.36 and 5.45 μM. The lead compound **9d** [N-(7-chloro-2-methylquinolin-4-yl)-N-(3-((diethylamino)methyl)-4-hydroxyphenyl)-2,3-dichlorobenzenesulfonamide] with null cytotoxicity (CC<sub>50</sub> > 300 μg/mL) and excellent anti-mycobacterial activity and selectivity (mycobacterium ATPase IC<sub>50</sub> = 0.51 μM, mammalian ATPase IC<sub>50</sub> > 100 μM, and selectivity > 200) exhibited a complete growth inhibition of replicating *Mycobacterium tuberculosis* H37Rv at 3.12 μg/mL. In addition, it also exhibited bactericidal effect (approximately 2.4 log<sub>10</sub> reductions in CFU) in the hypoxic culture of non-replicating *M. tuberculosis* at 100 μg/mL (32-fold of its MIC) as compared to positive control isoniazid [approximately 0.2 log<sub>10</sub> reduction in CFU at 5 μg/mL (50-fold of its MIC)]. The pharmacokinetics of **9d** after p.o. and IV administration in male Sprague–Dawley rats indicated its quick absorption, distribution and slow elimination. It exhibited a high volume of distribution (V<sub>ss</sub>, 0.41 L/kg), moderate clearance (0.06 L/h/kg), long half-life (4.2 h) and low absolute bioavailability (1.72%). In the murine model system of chronic TB, **9d** showed 2.12 log<sub>10</sub> reductions in CFU in both lung and spleen at 173 μmol/kg dose as compared to the growth of untreated control group of Balb/C male mice infected with replicating *M. tuberculosis* H37Rv. The in vivo efficacy of **9d** is at least double of the control drug ethambutol. These results suggest **9d** as a promising candidate molecule for further preclinical evaluation against resistant TB strains.

© 2015 Published by Elsevier Ltd.

## 1. Introduction

Tuberculosis, primarily caused by *Mycobacterium tuberculosis*, is one of the globally leading infectious disease that continues as global epidemic with more than 9 million new cases and nearly 2 million deaths every year.<sup>1</sup> In addition, over 2 billion people harbor latent TB infection (LTBI), thus representing an enormous reservoir of *M. tuberculosis* that can subsequently progress to active TB.<sup>1</sup> The main obstacles to the global TB control are: (i) the human

immunodeficiency virus (HIV) epidemic proven to increase the risk of developing active TB dramatically, (ii) the increasing emergence of multi-drug resistant TB (MDR-TB), extensively drug-resistant TB (XDR-TB) and a recently identified TB state called total drug-resistant TB (TDR-TB).<sup>1–5</sup> Current TB chemotherapy is mainly based on drugs that inhibit bacterial metabolism, and is characterized by efficient bactericidal and extremely weak sterilizing activities.<sup>6</sup> The dormant or latent or metabolically inactive bacilli are tolerant to the anti-TB drugs that target cell division.<sup>7,8</sup> Although an extended chemotherapy may be partially successful in eradicating such dormant bacilli, drug(s) with efficient sterilizing activity are of current demand for properly tackling the dormant bacilli. In such scenario, targeting the particular enzyme that are essential

☆ CDRI communication number allotted to this paper is 8882.

\* Corresponding author. Tel.: +91 (522) 2624273; fax: +91 (522) 2623938.

E-mail address: [anilsak@gmail.com](mailto:anilsak@gmail.com) (A.K. Saxena).

for the survival of both actively growing and latent/dormant bacilli, is one of the most effective target-based drug discovery approach.<sup>2</sup>

The mycobacterial  $F_0F_1$ -ATP synthase ( $F_0F_1$ -ATPase) is a validated anti-TB target, which is responsible for the production of adenosine 5'-triphosphate (ATP) for energy homeostasis in different mycobacterial species.<sup>9</sup> Bedaquiline (TMC207, Sirturo™) is a member of the diarylquinoline class of anti-TB drugs targeting this new enzyme and has been approved by the U.S. Food and Drug Administration (US-FDA) specifically for the treatment of MDR-TB. This drug has shown promising efficacy against both the drug-sensitive and drug-resistant TB, and has remarkable potential for restricting the duration of TB treatment due to the fact that this drug is bactericidal to both the replicating as well as non-replicating (dormant) bacilli.<sup>9–12</sup> Bedaquiline (Sirturo™) has been reported by the World Health Organization (WHO) to disturb the function of the heart and liver in particular. Common observed side effects include nausea, joint and chest pain, and headache.<sup>13</sup> Bedaquiline is proven to be a weak hERG (human Ether-à-go-go) potassium ( $K^+$ ) channel blocker (in vitro  $IC_{50} = 0.2 \mu\text{g/mL}$ ) that can cause prolongation of the heart QT interval (the time between the start of the Q wave and the end of the T wave in the heart's electrical cycle), thus disturbing normal function of the heart.<sup>14</sup> The observed efficacy of bedaquiline for the treatment of MDR-TB validates the target mycobacterial  $F_0F_1$ -ATPase, and the observed adverse events with this drug suggest further exploration of new chemical entities as selective  $F_0F_1$ -ATPase inhibitors lacking any potential adverse effects.

Structurally, the mycobacterial  $F_0F_1$ -ATPase is composed of a membrane-embedded  $F_0$  portion comprising  $a_1b_2c_{10-15}$  subunits and a hydrophilic  $F_1$  portion consisting of  $\alpha_3\beta_3\delta\epsilon$ .<sup>15</sup> Proton ( $H^+$ ) migration through  $F_0$  triggers the rotation of rotary ring formed by oligomeric subunits 'c' which is coupled to the rotation of the 'γ' subunit resided within the  $(\alpha\beta)_3$  hexamer of  $F_1$ . This biochemical phenomenon thus drives the synthesis of ATP as a source of energy for mycobacterium species. A high-resolution crystal structure of mycobacterial ATP synthase or its subunits is lacking till date. Computational and biological studies have shown that TMC207 binds at the interface of subunit 'a', and rotary subunits 'c'.<sup>15–17</sup> This drug is biochemically shown to interfere with the rotary movement of subunit 'c' by mimicking a conserved basic residue Arg186 in the subunit 'a' needed for the proton transfer with Glu61 of the subunit 'c'.<sup>16,17</sup> Through detailed computational studies, de Jonge and colleagues<sup>16</sup> reported the chiral *N,N*-dimethylpropanol substructure of TMC207 to exhibit H-bond formation with the carboxylate side chain of Glu61, and a favorable location of quinoline substructure at the interface of subunits 'a' and 'c' that might lead to blockade of the rotation of rotary ring, and thus normal interfering with the proton transfer cascade process. Haagsma et al.<sup>15</sup> have recently characterized the interaction between TMC207 and mycobacterial ATP synthase using biochemical assays and binding studies, where they have provided experimental support for ability of TMC207 to mimic a key residue Arg186 involved in the proton transfer cascade, and thus blocking rotary movement of subunits 'c' of the mycobacterial  $F_0F_1$ -ATP synthase.<sup>15,16</sup>

In view of the success of mycobacterial  $F_0F_1$ -ATP synthase as validated target for TB chemotherapy, we utilized the state-of-the-art medicinal chemistry approach for the identification of novel inhibitors of mycobacterial  $F_0F_1$ -ATP synthase. This effort led to invention of quinoline class of aryl-sulfonamides as potent, orally bioavailable and selective mycobacterial ATP synthase inhibitors that we have patented recently.<sup>18</sup> We have recently reported a short report on the biological screening of these compounds against *Mycobacterium smegmatis* ATP synthase along with in vitro testing against the dormant (non-replicating) *M. tuberculosis* H37Rv.<sup>12</sup> Herein, we report a full-length description of the rational design, synthesis and structure-activity relationship

(SAR) studies of these novel compounds proven as low micromolar inhibitors of the mycobacterial  $F_0F_1$ -ATP synthase. Among the synthesized series of 18 compounds, two lead compounds were biologically explored in greater detail where one representative compound was proven as an orally bioavailable and selective mycobacterium ATP synthase inhibitor that demonstrated approximately 2.12 log<sub>10</sub> reductions in CFU in both lung and spleen at a dose of 173  $\mu\text{mol/kg}$  as compared to the growth in the untreated control group of Balb/C male mice infected with *M. tuberculosis* H37Rv. Like the drug bedaquiline (Sirturo™, TMC207), this compound acts through a novel mechanism of action (ATP synthase), and is active against both the replicating as well as non-replicating *M. tuberculosis* H37Rv. This lead compound could be considered as candidate molecule for further preclinical evaluation that could lead to an effective TB therapeutics.

## 2. Materials and methods

### 2.1. Chemicals, reagents, culture media and test compounds

All of the chemicals, culture media, and reagents were purchased from common commercial suppliers. Solvents were purified and dried by standard procedures, when required. Chromatographic separations of the synthesized intermediates and title compounds were performed on silica gel (Merck: 100–200 mesh). Thin layer chromatography was used to monitor the progress and/or completion of the reactions. Melting points (uncorrected) were determined with Büchi 510 apparatus. Characterization of the synthesized compounds was accomplished in the sophisticated analytical instrument facility (SAIF) department of CSIR Central drug Research Institute, Lucknow (India). The IR spectroscopy was carried out using Perkin-Elmer 881 spectrophotometer and the values are expressed as  $\nu_{\text{max}} \text{ cm}^{-1}$ . Mass spectra (MS) were recorded on a Jeol (Japan) SX 102/DA-6000 Mass Spectrometer. <sup>1</sup>H NMR spectra were recorded on Bruker Spectrospin spectrometer at 300 MHz. The chemical shifts are reported in  $\delta$  scale (ppm) and are relative to tetramethyl silane (TMS) as internal standard. The coupling constants *J* are given Hertz and spin multiplicities are expressed s (singlet), d (doublet), t (triplet), dd (double doublet), and m (multiplet). The purity of final compounds was determined to be >95% by HPLC (high performance liquid chromatography).

### 2.2. Bacterial strains and growth conditions

*M. tuberculosis* H37Rv was maintained on Lowenstein Jensen slopes and freshly subcultured in the Middlebrook 7H9 medium (BD) containing 10% oleic acid-albumin-dextrose-catalase (OADC) and 0.05% Tween 80 maintained at 37 °C with shaking for 14–15 days to attain mid exponential phase (OD<sub>600</sub> ~0.6). *Mycobacterium smegmatis* TMC 607 was grown in the Luria Bertani broth containing 0.05% Tween 80 and 0.2% glycerol. These cultures were used for downstream experiments.

### 2.3. Preparation of inverted membrane vesicles

Inverted membrane vesicles of *M. smegmatis* were prepared according to methods described elsewhere.<sup>10,12</sup> The reversed membrane fraction was resuspended in an appropriate volume of 50 mM MOPS buffer (pH 7.5) containing 2 mM  $\text{MgCl}_2$  and 1 mM PMSF. The protein content was estimated using the Bradford method. The vesicle preparation was stored as aliquots at –80 °C. For the assay, membrane vesicles were diluted to a concentration of 100  $\mu\text{g}$  protein/mL with 50 mM MOPS buffer (pH 7.5) containing 10 mM  $\text{MgCl}_2$ .

## 2.4. Assay for inhibition of mycobacterial ATP synthase

The inhibition of ATP synthesis was measured according to methods described elsewhere.<sup>10,12</sup> The membrane vesicles were preincubated with test compounds at two fold serial dilutions ranging from 50  $\mu$ M to 0.39  $\mu$ M or *N,N'*-dicyclohexylcarbodiimide (DCCD) at 100  $\mu$ M or isoniazid (INH) at 0.3  $\mu$ M under stirring condition at room temperature for 10 min. Subsequently 2.5 mM NADH was added and further incubated with vigorous shaking for 1 min. The reaction was started by addition of 1 mM ADP and 10 mM potassium phosphate. After incubation for 1 h, aliquots (0.05 mL) were added to 0.2 mL of stock solution (2 mM EDTA, 1% trichloroacetic acid). 0.005 mL of this mixture was added to 0.1 mL tris acetate buffer (100 mM Tris, 2 mM EDTA, pH 7.75) in a 96 well plate. After addition of 0.1 mL luciferase reagent (Promega Bactiter-Glo), luminescence was measured using a luminometer (BMG POLARstar Galaxy Microplate reader). The concentration causing 50% inhibition of ATP synthesis ( $IC_{50}$ ) was determined after plotting concentration values of test sample(s) against percent inhibition of ATP synthesis.

## 2.5. Determination of MICs against *M. tuberculosis* H37Rv

Agar dilution assay<sup>19</sup> was used to determine the minimum inhibitory concentration (MIC) of test compounds. Test compounds were dissolved in dimethylsulfoxide (DMSO) to make 5 mg/mL stock solutions. Serial dilutions from stocks were also made in DMSO. Standard anti-TB drug INH was used as positive control and the vehicle (DMSO) was used as negative control. An amount of 0.1 mL of serially diluted test compounds or standard drugs were added to 1.9 mL Middlebrook 7H10 agar medium (with OADC supplement, in glass tubes). DMSO (0.1 mL/tube) was used as vehicle control. The contents were mixed and allowed to solidify as slants. Three-week old culture of *M. tuberculosis* H37Rv was harvested from Lowenstein-Jensen medium and its suspension (1 mg/mL, equivalent to  $10^8$  bacilli) was made in normal saline containing 0.05% Tween-80. 10  $\mu$ L of 1:10 dilution of this suspension ( $\sim 10^5$  bacilli) was inoculated into each tube and incubated at 37 °C for 4 weeks. The lowest concentration of the compound up to which there was no visible growth of bacilli was its MIC.

## 2.6. Estimation of ATP synthesis inhibition in whole *M. tuberculosis* H37Rv

The culture of *M. tuberculosis* H37Rv was declumped by bead-vortexing settling method and the resulting supernatant was adjusted to turbidity equivalent to ~McFarland #1 standard. This was further diluted 100-fold and dispensed as 1 mL volumes microfuge tubes containing 0.5 mm glass beads. Different concentrations of the test compounds were added and incubated for 18 h at 37 °C. ATP synthesis in treated and untreated cultures were determined by method described elsewhere,<sup>8</sup> with some modifications. The samples were heated for 8–10 min and cooled on ice and then lysed in a bead beater. Cell debris was removed by centrifugation and ATP content in the lysate was measured by Luciferase based assay (Promega Bactiter-Glo).

## 2.7. Determination of bactericidal activity in non-replicating hypoxic culture of *M. tuberculosis*

The non-replicating hypoxic culture of *M. tuberculosis* H37Rv (Wayne model) was prepared as described elsewhere.<sup>6,20</sup> In brief, a mid log phase culture of the bacilli in Middlebrook 7H9 broth was diluted to approximately 105 cfu/mL and dispensed as 10 mL volumes into head space vials of 20 mL capacity containing magnetic beads. Methylene blue 1.5  $\mu$ g/mL was added to the two tubes

as indicator for oxygen depletion. The vials were incubated at 37 °C on a magnetic stirrer with slow stirring for 20–22 days or until methylene blue was decolorized. The two standard drugs isoniazid (INH) and rifampicin (RIF) were tested at 0.5 and 5  $\mu$ g/mL, while thioridazine at 5 & 50  $\mu$ g/mL, metronidazole at 50  $\mu$ g/mL and DCCD at 100  $\mu$ M. The test compounds were tested at the two doses 10 and 100  $\mu$ g/mL. All the drugs as well as compounds were tested in duplicates. Appropriate concentration of the test compound/standard drug was added to respective vials by injection through septa and the vials were further incubated at 37 °C for 4 days. The total CFU counts of serial dilutions were performed on Middlebrook 7H10 (MB7H10) agar plates.

## 2.8. Inhibition of mitochondrial ATP synthase

Mouse liver mitochondria were isolated using the protocol described by Frezza et al.<sup>21</sup> In brief, an adult Swiss mouse (3 months old) was starved overnight and then euthanized by cervical dislocation prior to dissecting out the liver. The liver was minced and homogenized (glass-teflon potter at 1600 rpm, 4 strokes) in ice cold buffer (200 mM sucrose, 10 mM Tris-MOPS and 1 mM EGTA-Tris, pH7.4). The homogenate was then centrifuged at 600 rpm for 10 min at 4 °C to remove unbroken cells and debris. The supernatant was further centrifuged at 7000 rpm for 10 min at 4 °C. The pellet was washed once with ice-cold buffer. The supernatant was discarded and the mitochondrial pellet was resuspended in residual supernatant in the tube and stored at –80 °C. The protein content was estimated by the Bradford method. The ATP synthesis by the mitochondria was assayed on the same day as isolation by method described elsewhere<sup>22</sup> with some modifications. Briefly, 100  $\mu$ g of mitochondria were incubated at room temperature with vigorous stirring in the presence of 100  $\mu$ M compounds/DCCD in 20 mM Tris/HCl, 0.15 M sucrose, 5 mM  $MgCl_2$ , 100  $\mu$ M diadenosine pentaphosphate at pH 7.4. Reactions were started by adding 1 mM ADP, 20 mM Pi and 50 mM succinate and arrested after 1 h with 2 mM EDTA-1% TCA. The amount of ATP formed was measured similar to the method described above for mycobacterial ATP synthase assay.

## 2.9. In vitro cytotoxicity

The compounds were tested in an in vitro model for cytotoxicity with Vero monkey kidney cells using Resazurin assay.<sup>23</sup> The Vero cells (ATCC CCL-8 1) were seeded overnight at  $1 \times 10^4$ – $3 \times 10^6$  cells per well in 96-well plates at 37 °C in RPMI supplemented with 10% heat-inactivated fetal bovine serum and 5% CO<sub>2</sub>. Cells were exposed to dilutions of experimental and control drugs in triplicate for 2 h with each compound at a range of concentrations from 100–1.56  $\mu$ g/mL. Rifampicin was used as a control at the same concentrations. Each well had 100  $\mu$ L of the test material in serially descending concentrations. After 72 h of incubation, 10  $\mu$ L of Resazurin indicator solution (0.1%) was added and incubation was continued for 4–5 h. Any color change from purple to pink or colorless was recorded as positive. Fluorescence was measured of each sample with excitation wavelength at 530 nm and emission wavelength at 590 nm using the BMG Polar Star Galaxy. The CC<sub>50</sub> values (50% inhibitory concentrations) were calculated by plotting fluorescence values using Microsoft excel template. The data from this toxicity testing and MIC values were used to calculate a selectivity index (SI), the ratio of CC<sub>50</sub>: MIC.

## 2.10. In vivo cytotoxicity

The compounds were also tested in an in vivo model for cytotoxicity with mouse bone marrow derived macrophages using the method described elsewhere.<sup>24</sup> [Please note: Prior undertaking

the *in vivo* experiments in mouse model system, a permission of the institute's ethics committee (CPCSEA registration number 34/1999 dated 11.3.99, extended up to 2012) had been taken]. Mouse was euthanized by exposure to CO<sub>2</sub> and the femur bones were dissected out. The bones were trimmed at each end, and the marrow was flushed out (using 26-gauge needle) with 5 mL of Dulbecco's minimal essential medium (DMEM) supplemented with 10% FBS, 15% L-929 fibroblast conditioned supernatant (prepared as described later), and non-essential amino acids. Cells were washed twice and plated in 96-well tissue culture plates at a concentration of 105 cells per well (100 mL) in supplemented DMEM. The monolayers were then incubated at 37 °C in 5% CO<sub>2</sub>. After 48 h, 20 mL of MTS solution was added to each well and incubated for 2 h at 37 °C in 5% CO<sub>2</sub>. Reading was taken at 490 nm using a plate reader. Absorbance shown by DMSO containing wells was taken as 100% survivors. A compound was considered toxic if it causes 50% inhibition at a concentration 10-fold higher than its MIC.

## 2.11. Pharmacokinetic (PK) studies

The PK studies was carried out in young and healthy male Sprague–Dawley rats weighing 250 ± 25 g. The study was conducted in three rats per time point. In all experiments, euthanasia and disposal of carcasses were carried out as per the guidelines of Local Ethics Committee for animal experimentation. All pharmacokinetic parameters were calculated by two compartmental models using the WinNonlin program, version 5.1 (Scientific Consulting Inc.). The experimental detail of the PK studies is provided in supporting information.

## 2.12. *In vivo* anti-tubercular activity

Compounds were tested in a murine model of chronic TB.<sup>25</sup> a well known model for evaluation of new anti-TB drugs and combinations. Balb/C mice (8–10 week-old) of average weight (18–20 g) were infected intravenously with 0.2 mL of a freshly prepared bacterial suspension containing ~5 × 10<sup>6</sup> CFU of *M. tuberculosis* H37Rv. There were ten mice in each group and 10 mice were kept as untreated control. The drugs were administered by an esophageal cannula (gavage) six times weekly started on day 1 and continued for 4 weeks. The treated mice were administered one of the following treatments INH at 25 mg/kg, ethambutol (EMB) at 100 mg/kg, compound **9d** at 100 mg/kg and 50 mg/kg and compound **9e** at 100 mg/kg of body weight. The severity of infection and the effectiveness of the treatments were assessed by the 30-day survival rate, CFU per spleen and per lung. The last doses were administered on day D28 and all surviving mice were sacrificed on

D30, plated on MB7H10 containing OADC and incubated at 37 °C for 4–6 weeks.

## 3. Results

### 3.1. Rational design and structure-based optimization

Through detailed computational studies, de Jonge and colleagues reported the important structural features in TMC207 governing its ATP synthase inhibitory activity.<sup>16</sup> They reported the chiral *N,N*-dimethylpropanol substructure to exhibit H-bond formation with the carboxylate side chain of Glu61 residue, and the favorable binding of the quinoline substructure at the interface of subunits 'a' and 'c' of the mycobacterium F<sub>0</sub>F<sub>1</sub>-ATP synthase. In view of this, we carried out the preliminary database screening of the Asinex database keeping in view the three important structural features, namely quinoline, tertiary amine and hydroxyl function present in bedaquiline (TMC207), which led to the identification of amodiaquine (BAS 00327385) (Fig. 1). Despite of the presence of these features, amodiaquine is not known to inhibit the ATP synthase enzyme. This knowledge prompted us to embark on structure-based studies using the *in house* developed homology model of mycobacterial ATP synthase using the NMR structure *Escherichia coli* ATP synthase.<sup>26</sup> Computational detail is given as the [Supplementary data](#). In brief, the molecular docking study revealed that one of the possible reasons behind the lack of ATP synthase inhibitory activity of amodiaquine may be the absence of hydrophobic pocket attached to the NH group of amodiaquine, corresponding to the naphthyl group of TMC207 that could occupy the deep hydrophobic pocket (Fig. 2). Therefore, we docked several new analogues containing hydrophobic groups like aryl (Ar), ArCH<sub>2</sub>, ArCO, ArSO<sub>2</sub>, etc, substituted to the NH center. The docking experiment revealed the particular suitability of aromatic sulfonamide substructure to favorably occupy this extended pocket (Fig. 2D). The sulphonyl group aided further H-bond interactions with the surrounding polar residues (described in the later section). In addition, a methyl group as a replacement of the methoxy group of the amodiaquine was done in order to simulate the steric effect as suggested by the docking studies. With this new designed prototype (compound **8**), we synthesized a novel series of aryl sulfonamide derivatives (Table 1) for biological screening using both *in vitro* enzyme-based as well as whole cell assays.

### 3.2. Chemistry

Compounds were prepared using steps as illustrated in Schemes 1–3. The reaction of *m*-chloroaniline (**1**) with the

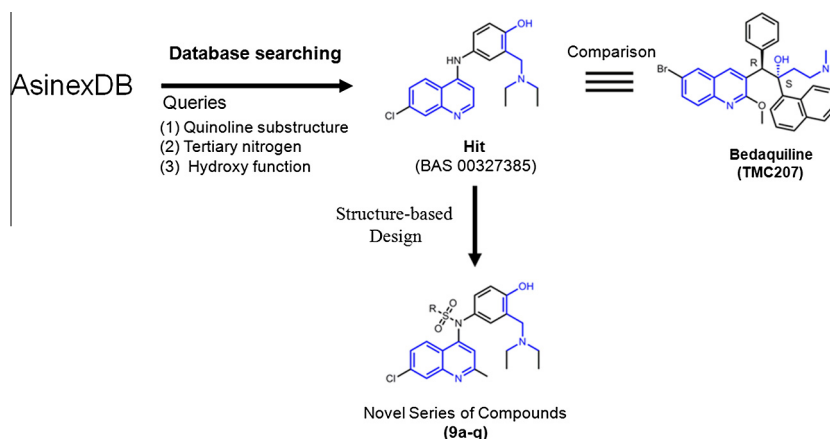
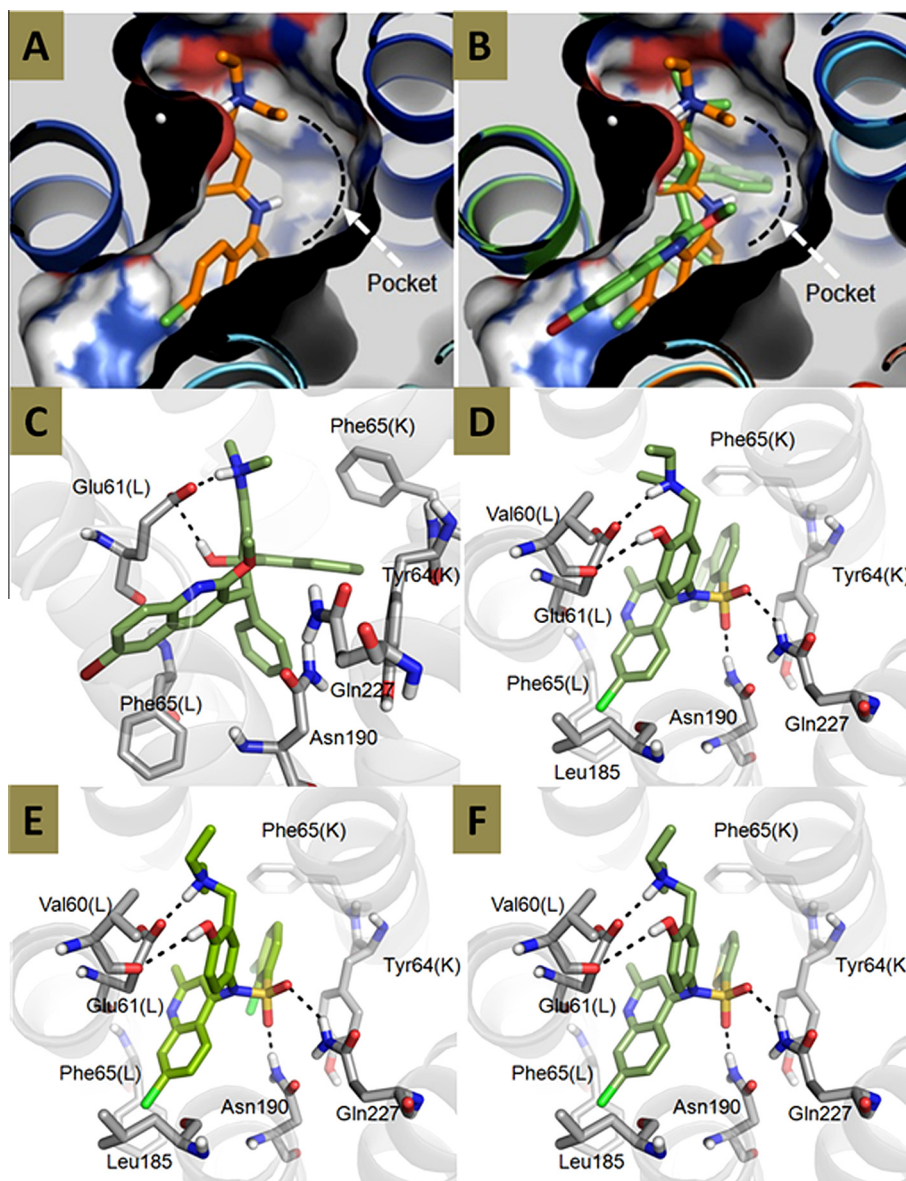


Figure 1. Scheme adopted for the design of new ATP synthase inhibitor.





**Figure 2.** (A) The binding pattern of the hit BAS 00327385 into the active site of homology modeled *M. tuberculosis* ATPase. (B) The comparison of the binding poses of the potential hit BAS 00327385 (amber colored) and bedaquiline (TMC207) (green colored) into the active site of homology modeled ATPase. Arrow indicates the unoccupied hydrophobic pocket beneath the NH group of the hit BAS 00327385, which is occupied by the naphthalene motif of the TMC207. The binding mode of (C) bedaquiline or TMC207, (D) compound **9l**, (E) compound **9d** and (F) compound **9p** into the active site of homology modeled ATP synthase. Important active site residues are labeled and shown as grey colored sticks. The protein is depicted as cartoon. The letters 'K' or 'L' in the parentheses of residue numbers depict the protein chain of the mycobacterial ATPase.

ethylacetoacetate in the presence of catalytic amount of hydrogen chloride (HCl), followed by heating under reflux using phenyl ether afforded the intermediate compound **2**. The intermediate **2** was then treated with phosphorous oxychloride ( $\text{POCl}_3$ ) that afforded the intermediate compound **3** (Scheme 1).

On the other hand, the reaction of *p*-anisidine (**4**) with acetic anhydride in the presence of sodium acetate as a base, under reflux, afforded the intermediate compound **5**. This intermediate **5** upon treatment with molar solution of boron tribromide ( $\text{BBr}_3$ ) in dichloromethane (DCM) afforded the intermediate compound **6**. Finally, the reaction of the intermediate **6** with formaldehyde and diethylamine under reflux in absolute ethanol using catalytic amount of acetic acid afforded the desired intermediate compound **7** (Scheme 2).

In the next stage, syntheses of compound **8** and final title compounds (**9a–q**) were accomplished using the above synthesized

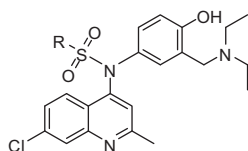
intermediates (**3** and **7**) as outlined in Scheme 3. The reaction of the intermediate compounds **3** and **7** in presence of 20% HCl followed by the refluxing in absolute ethanol afforded the compound **8**. Finally, the compound **8** was treated with different substituted/ unsubstituted aliphatic/ alicyclic/ aromatic/ heteroaromatic sulfonyl chloride in the presence of *N,N*-diisopropylethyl amine (DIPEA) as inorganic base, and acetone as solvent to afford title compounds **9a–q**.

### 3.3. Inhibition of *M. smegmatis* ATP synthase

The ATP synthase inhibitory activity of the synthesized title compounds (**8**, **9a–q**) was determined in the inverted membrane vesicles isolated from *M. smegmatis* using the method described elsewhere.<sup>10</sup> The DCCD adduct was used as positive control,

**Table 1**

In vitro ATP synthase inhibitory activity ( $IC_{50}$ ,  $\mu M$ ) of synthesized compounds (**8**, **9a–q**), DCCD (positive control) and INH (negative control) evaluated in the inverted membrane vesicles isolated from *M. smegmatis*



Title	R	<i>M. smegmatis</i> ATP synthase $IC_{50} \pm SEM$ ( $\mu M$ )
<b>8</b>	N/A	$5.45 \pm 0.264$
<b>9a</b>		$0.53 \pm 0.015$
<b>9b</b>		$0.74 \pm 0.021$
<b>9c</b>		$0.39 \pm 0.017$
<b>9d</b>		$0.51 \pm 0.030$
<b>9e</b>		$0.63 \pm 0.135$
<b>9f</b>		$1.34 \pm 0.155$
<b>9g</b>		$1.26 \pm 0.180$
<b>9h</b>		$1.36 \pm 0.352$
<b>9i</b>		$1.83 \pm 0.453$
<b>9j</b>		$1.04 \pm 0.024$
<b>9k</b>		$3.29 \pm 0.091$
<b>9l</b>		$1.00 \pm 0.031$
<b>9m</b>		$0.92 \pm 0.157$
<b>9n</b>		$1.85 \pm 0.489$
<b>9o</b>		$1.57 \pm 0.300$
<b>9p</b>		$0.36 \pm 0.303$
<b>9q</b>		$3.41 \pm 0.465$
DCCD		$99.5 \pm 3.53\%$ inhibition at $100 \mu M$

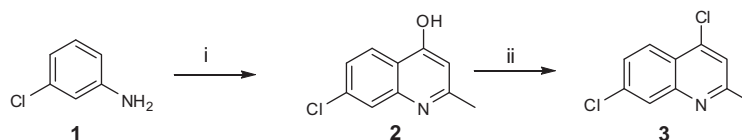
whereas INH was used as a negative control in this assay. The experimentally determined *M. smegmatis* ATP synthase inhibitory activities ( $IC_{50}$ ,  $\mu M$ ) of the tested compounds (**8**, **9a–q**) along with positive and negative controls are summarized in Table 1.

### 3.4. Structure–activity relationships

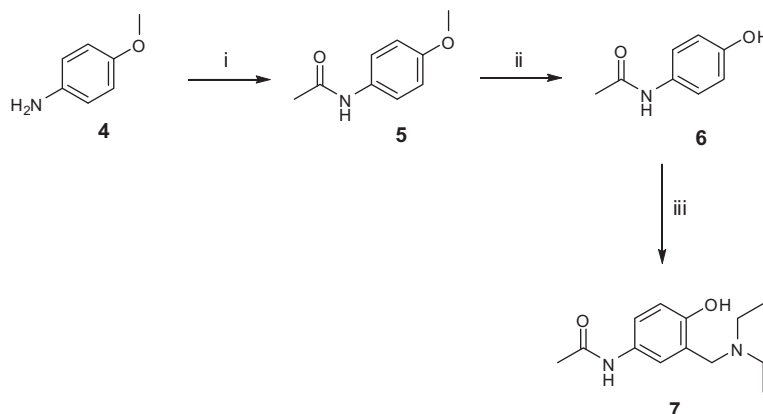
The synthesized compounds (**8**, **9a–q**) exhibited potent inhibition of *M. smegmatis* ATP synthase activity with  $IC_{50}$  values ranging from 0.36 to 5.45  $\mu M$ , while the positive control DCCD showed  $99.5 \pm 3.53\%$  inhibition at 100  $\mu M$  concentration. In this assay, the negative control INH did not show any significant inhibition (0% inhibition at 0.3  $\mu M$ ), thus validated the reliability of the assay system (Table 1). The sulfonamide derivatives (**9a–q**) exhibited potent inhibition of *M. smegmatis* ATP synthase better than the non-sulfonamide precursor **8**, and thus validated our computational insights of the suitability of hydrophobic groups linked to the NH group at 4th position of quinoline for effective binding within the hydrophobic pocket as shown by an arrow in Figure 2. The compound **9p** ( $IC_{50} = 0.36 \mu M$ ) possessing 5-chlorothiophene-2-sulfonyl group was the most potent compound in the series, and the compound **9b** ( $IC_{50} = 0.39 \mu M$ ) possessing 4-nitrobenzene sulfonyl group at the corresponding position exhibited almost comparable ATP synthase inhibition.

Among the mono/di-substituted chlorobenzene sulfonyl derivatives (**9a**, **9d–g**), the three compounds **9a** ( $IC_{50} = 0.53 \mu M$ ), **9d** ( $IC_{50} = 0.51 \mu M$ ) and **9e** ( $IC_{50} = 0.63 \mu M$ ) exhibited about 2-fold better inhibition than compounds **9f** ( $IC_{50} = 1.34 \mu M$ ) and **9g** ( $IC_{50} = 1.26 \mu M$ ). The binding mode of the compound **9d** at the active site of ATP synthase (Fig. 2E) revealed that the 2,3-dichlorophenyl moiety occupy the deep hydrophobic pocket corresponding to the naphth-1-yl substructure of the TMC207, where sulfonyl oxygen form two direct H-bonds with the Asn190 and Gln227 residues (located in the subunit 'a'). Similar to TMC207, the protonated tertiary amine and hydroxyl group of this compound participated in H-bond formation with the carboxylate oxygen of Glu61(L) and backbone amidic keto of the Val60(L) residues. Unlike the compound **9p**, compound **9o** ( $IC_{50} = 1.57 \mu M$ ) lacking chloro group at 5th position of thiophene exhibited about 5-fold lower ATPase inhibitory activity. This in turn substantiates particular importance of the chlorothiophene group for stronger hydrophobic interaction in this region for better binding and inhibition. This inference was well substantiated by docking study, where the chloro group of the compound **9p** exhibited hydrophobic interaction with Phe65(K) and Leu68(K) residues (Fig. 2F).

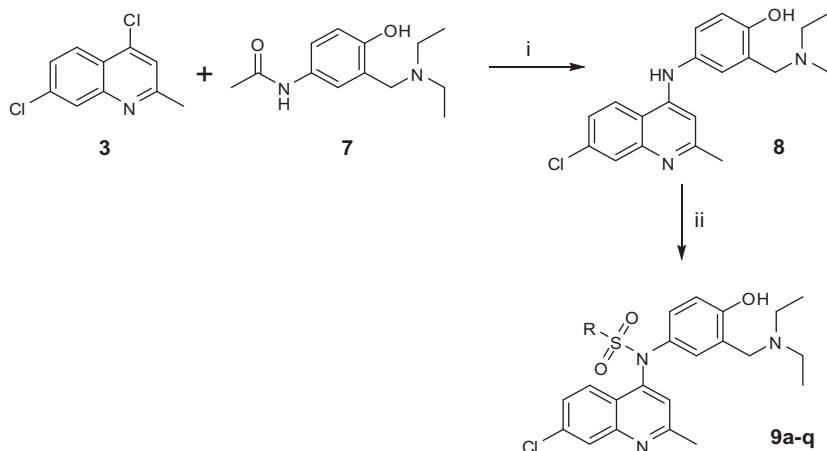
Among the compounds **9l–n** possessing bicyclic aromatic sulfonyl groups (Table 1), the compounds **9l** ( $IC_{50} = 1.00 \mu M$ ) and **9m** ( $IC_{50} = 0.92 \mu M$ ) exhibited about 2-fold better inhibition than the compound **9n** ( $IC_{50} = 1.85 \mu M$ ). Although, the observed ATPase inhibitory activities of these two compounds (**9l** and **9m**) were lower than compounds **9a–e** and **9p** possessing substituted monocyclic aromatic sulfonyl groups, but still were comparable to the compound **9j** ( $IC_{50} = 1.04 \mu M$ ) comprising 2,4,6-trimethylbenzene sulfonyl group. The compound **9q** ( $IC_{50} = 3.41 \mu M$ ) having a fused alicyclic sulfonyl group, exhibited poor ATPase inhibition compared to those compounds possessing aromatic sulfonyl groups (**9a–p**). This may be attributed to the greater bulk of the fused alicyclic group, and thus suggested the importance of aromatic group at this position for better accommodation into the aforementioned extended hydrophobic pocket. Altogether, it may be concluded that the most noticeable feature among the studied series of aromatic sulfonamides essential for the ATP synthase inhibitory



**Scheme 1.** Synthesis of the intermediate compound **3**. Reagents and conditions: (i) (a) ethylacetoacetate, HCl; (b) phenyl ether, 190 °C, 1 h (ii) POCl<sub>3</sub>.



**Scheme 2.** Synthesis of the intermediate compound **7**. Reagents and conditions: (i) acetic anhydride, sodium acetate, reflux; (ii) BBr<sub>3</sub>, DCM; (iii) formaldehyde, diethylamine, acetic acid, ethanol.



**Scheme 3.** Synthesis of the compounds **8** and **9a–q**. Reagents and conditions: (i) (a) 20% HCl (b) ethanol, reflux (ii) sulfonyl chloride, DIPEA, acetone.

activity is the presence of aromatic sulfonyl group attached to the NH of the compound **8** for better accommodation and binding within the an extended hydrophobic pocket, and hence needed for better inhibition of mycobacterial ATP synthase enzyme.

### 3.5. Growth inhibition of whole *M. tuberculosis* H37Rv

A set of eight compounds (**9a–e**, **9l**, **9m** and **9p**) with proven ATP synthase inhibitory activities ( $IC_{50} \leq 1 \mu M$ ), were further screened in the whole cell assay system against *M. tuberculosis* H37Rv using the agar dilution assay. The antimycobacterial spectrum of these compounds against the whole *M. tuberculosis* H37Rv strain are summarized in Table 2, where MIC ( $\mu g/mL$ ) represents the minimum inhibitory concentration causing complete (100%) growth inhibition of the *M. tuberculosis* H37Rv strain. The two compounds **9d** and **9e** with promising ATP synthase inhibitory activities ( $IC_{50} \sim 0.5 \mu M$ ) exhibited the 100% (complete) inhibition of *M. tuberculosis* H37Rv at the lowest concentration, that is,

3.12  $\mu g/mL$  each, whereas the other three compounds **9a**, **9c** and **9p** exhibited complete inhibition at 2-fold higher concentration of 6.25  $\mu g/mL$ . Other compounds were moderately active ( $MIC \geq 12.5 \mu M$ ).

### 3.6. Cytotoxicity

The four potent compounds (**9a**, **9c–e**) were evaluated for any cytotoxicity using an in vitro assay described by Anoopkumar-Dukie et al.<sup>23</sup> using the Vero monkey cells, and an in vivo assay described by Mosmann<sup>24</sup> using mouse bone marrow derived macrophages. The experimentally determined  $CC_{50}$  ( $\mu g/mL$ ) values and selectivity index (SI) of these compounds using in vitro assay are summarized in Table 2. The  $CC_{50}$  values of the three compounds **9a**, **9d** and **9e** were  $>300 \mu g/mL$  whereas for compound **9c** was 55  $\mu g/mL$ . The selectivity index ( $SI = CC_{50}/MIC$ ) which is an indicator of therapeutic window, was highest for the compound **9d** ( $>98$ ) and lowest for the compound **9c** (17.55). The SI values for other

**Table 2**Antimycobacterial spectrum (in vitro) of the selected compounds against whole *M. tuberculosis* H<sub>37</sub>Rv strain

Title	<i>M. tuberculosis</i> H <sub>37</sub> Rv growth inhibition MIC (μg/mL)	Vero cell CC <sub>50</sub> (μg/mL)	Selectivity index (SI)
<b>8</b>	>50	ND	ND
<b>9a</b>	6.25	>300	>48
<b>9b</b>	>12.5	ND	ND
<b>9c</b>	6.25	55	18
<b>9d</b>	3.12	>300	>96
<b>9e</b>	3.12	>300	>48
<b>9i</b>	12.5	ND	ND
<b>9m</b>	>25	ND	ND
<b>9p</b>	6.25	ND	ND
INH	0.1	ND	ND

two compounds (**9a** and **9e**) were greater than 48. In addition, these compounds were non-toxic in the in vivo assay conducted using the mouse bone marrow derived macrophages. Therefore, the two compounds **9d** and **9e** were selected as candidate molecules for further investigation.

### 3.7. Fall in cellular ATP level in whole *M. tuberculosis*

The culture of *M. tuberculosis* H37Rv was exposed to the test compounds/drugs for 18 h in order to estimate the decline in total cellular ATP content, which is shown in Figure 3A. Bacilli treated with INH and RIF at 0.5 μg/mL (5-fold of their MICs) led to 78.5% and 69.6% fall in total cellular ATP level respectively, while 100 μM concentration of DCCD caused 30% fall in total ATP level, most of which probably may be generated by substrate level phosphorylation in live cells. On the contrary, bacilli treated with the two lead compounds **9d** and **9e** led to about 31 and 26% fall in total cellular ATP level, respectively at 50 μg/mL (approx. 15 fold of their MICs), and approximately 60% and 54% fall at 12.5 μg/mL (4-fold of

their MICs). These results indicate that these compounds do reduce the amounts cellular ATP produced by ATP synthase and hence cause ATP levels to fall faster than by INH/RIF.

### 3.8. Selectivity towards mycobacterial ATP synthase

The ATP synthase is a universal enzyme, and hence the selectivity towards mycobacterial ATP synthase is crucial for an anti-TB drug acting through this pathway.<sup>2</sup> In order to elucidate the selectivity of the lead compounds toward mycobacterial ATP synthase, the lead compounds **9d** and **9e** along with DCCD, INH and RIF were evaluated against mitochondrial ATP synthase obtained from mouse liver. In this experiment, DCCD showed 83% inhibition, while the lead compounds (**9d** and **9e**) showed only 5–10% inhibition of the mitochondrial ATP synthase at 100 μM, thus suggesting the identified lead compounds to be highly selective (selectivity >155) towards mycobacterial ATP synthase (Table 3).

### 3.9. Bactericidal activity against non-replicating (Dormant) *M. tuberculosis*

Since ATP synthase is crucial for the survival of mycobacteria during non-replicating persistence, the two lead compounds (**9d** and **9e**) were also tested against non-replicating *M. tuberculosis* H<sub>37</sub>Rv in Wayne Model under hypoxic/(oxygen depleted) condition considering INH as negative and metronidazole (MTZ) as positive controls. The lead compound **9d** exhibited bactericidal effect in the hypoxic culture of *M. tuberculosis* at 100 μg/mL (32-fold of its MIC), and showed more than 2.3 log<sub>10</sub> reductions in CFU while the lead compound **9e** showed about 1.5 log<sub>10</sub> reductions in CFU (Table 3). In this assay, the negative control INH showed only approximately 0.2 log<sub>10</sub> reduction in CFU at 5 μg/mL (100 fold of its MIC), and MTZ showed approximately 1 log<sub>10</sub> reduction in CFU at 50 μg/mL (Table 3). These results further support the

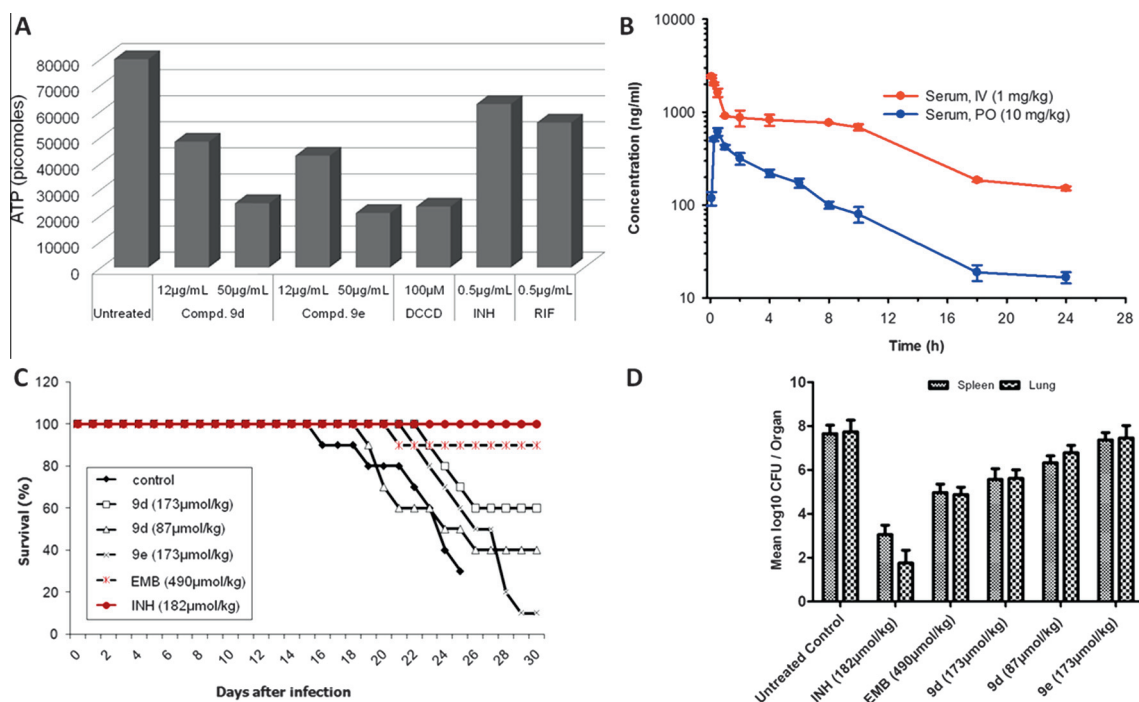


**Figure 3.** (A) Effect of lead compounds on total cellular ATP content of *M. tuberculosis* H37Rv. (B) Concentration-time profile of the lead compound **9d** after a single oral (10 mg/kg) and intravenous (1 mg/kg) dose in male Sprague–Dawley rats. Bar represents the standard error of mean (SEM). (C) Survival rate of mice for 30 days after intravenous infection of *M. tuberculosis* H37Rv. (D) Mean log<sub>10</sub> CFU per spleen and lungs of mice after 30 days post-treatment with test compound **9d** and drugs (INH and EMB). Mice were infected intravenously with  $5 \times 10^6$  CFU of *M. tuberculosis* H37Rv, and treatment was begun the next day after infection. There were 10 mice in each group. Untreated control mice did not receive any treatment. Error bars represent standard deviations.



**Table 3**Selective inhibition of mycobacterial versus mammalian ATP synthase and bactericidal activity against dormant bacilli by lead compounds **9d** and **9e**

Compd	<i>M. smegmatis</i> ATPase IC <sub>50</sub> (μM) or % inhibition at 100 μM	Mammalian ATPase IC <sub>50</sub> or % inhibition at 100 μM	<i>M. tuberculosis</i> H37Rv MIC (μg/mL) (ADA)	Bactericidal activity against non-replicating <i>M. tuberculosis</i> H37Rv in hypoxic culture		
				Concn (μg/mL)	Fold of MIC	Log <sub>10</sub> reduction in CFU/mL
<b>9d</b>	0.51 ± 0.030	>100 μM	3.12	100	32	2.34 ± 0.41
				10	3.2	1.14 ± 0.17
<b>9e</b>	0.63 ± 0.135	>100 μM	3.12	100	32	1.64 ± 0.14
				10	3.2	0.79 ± 0.24
INH	NA	NA	≤0.12	5	100	0.21 ± 0.08
MTZ	NA	NA	NA	50	NA	1.16 ± 0.16
DCCD	99.5%	83%	NA	100	NA	4.68 ± 0.08

inhibitory property of the lead compounds (**9d** and **9e**) for mycobacterial ATP synthase, as reflected by their effect on bacterial viability under microaerophilic/dormant conditions.

### 3.10. Activity against bacteria and fungi

The two lead compounds (**9d** and **9e**) were evaluated up to 50 μg/mL concentration each against both bacteria [*E. coli* (ATCC-9637), *Staphylococcus aureus* (ATCC-25923), *Klebsiella pneumonia* (ATCC-27736), and *Pseudomonas aeruginosa* (ATCC BAA-427)] as well as fungi [*Candida albicans*, *Cryptococcus neoformans*, *Sporothrix schenckii*, *Trichophyton mentagrophytes*, *Aspergillus fumigatus*, *Candida parapsilosis* (ATCC-22019)]. As expected, these lead compounds did not show any inhibition of both bacteria as well as fungi at the maximum concentration of 50 μg/mL (details are given in [Supplementary material](#)). This may be considered as an added advantage for anti-TB drug which are given for longer duration than other infections and hence, it is required that such molecule should not have any antibacterial or antifungal activity which may lead to the development of resistance against both bacteria (Gram-positive and Gram-negative) and fungi.

### 3.11. Pharmacokinetic studies

Pharmacokinetic studies on the lead compound **9d** revealed that the animals well tolerated the treatment as no peculiarities in the animal behavior were observed. This compound was rapidly absorbed and slowly eliminated ([Fig. 3B](#) and [Table 4](#)). Following oral dose, the observed maximum plasma concentration ( $C_{\max}$ ) and the time to reach the maximum plasma concentration ( $t_{\max}$ ) values suggested that the compound is mainly absorbed from the stomach. The volume of distribution ( $V_{ss}$ , 0.41 L/kg) of compound **9d** is greater than the total blood volume (0.054 L/kg)<sup>24</sup> indicating high extra-vascular distribution of the compound. The systemic clearance of compound **9d** was smaller than the hepatic blood flow of the rat (2.9 L/h/kg),<sup>24</sup> suggesting an insignificant amount of extra-hepatic elimination of the compounds. Moreover, low clearance (0.06 L/h/kg) of this compound suggests a potentially long acting profile (6.69 h based on MRT<sub>p.o.</sub>).

### 3.12. In Vivo antimycobacterial activity

The lead compound **9d** with potent ATP synthase inhibitory activities ([Table 1](#)) and growth inhibitory activity against both replicating as well as non-replicating whole *M. tuberculosis* ([Table 2](#)), was evaluated in a murine model of chronic TB<sup>25</sup> using the Balb/C mice (8–10 week-old) of average weight (18–20 g). In this assay, INH and EMB were used as positive controls. The compound **9d** was administered at the two dose levels, that is, 87 and 173 μmol/kg (i.e., 50 and 100 mg/kg, respectively) of body weight

**Table 4**Pharmacokinetic parameters of the compound **9d** in male Sprague–Dawley rats<sup>a</sup>

Parameters	Compound <b>9d</b>	
	Oral	Intravenous
$C_{\max}$ (ng/ml)	616.09 ± 58.11	2416.89 ± 92.46
$t_{\max}$ (h)	0.5	0.0833
AUC (ng h/ml)	2813	16393
$t_{1/2}$ (h)	4.20	8.84
$V_{ss}$ (L/kg)	0.41	0.84
Clearance (L/h/kg)	0.06	0.07
Bioavailability (%)	1.72	—

<sup>a</sup> Each value represents the average of three rats dosed orally (10 mg/kg) and intravenously (1 mg/kg); values of  $C_{\max}$  are mean ± SEM; AUC = area under the serum concentration-time curve,  $C_{\max}$  = serum peak concentration,  $t_{\max}$  = time to  $C_{\max}$ ,  $t_{1/2}$  = elimination half-life,  $V_{ss}$  = volume of distribution.

each in the two separate groups of mice, whereas the two positive controls (INH and EMB) were administered at fixed doses of 182 and 490 μmol/kg (i.e., 25 and 100 mg/kg, respectively) of body weight respectively through an esophageal cannula (gavage) six times weekly started on day 1 and continued for 4 weeks. The severity of infection and the effectiveness of the treatments were assessed by the 30-day survival rate, CFU per spleen and per lung. The survival rates of mice for 30 days after intravenous infection with  $5 \times 10^6$  CFU of *M. tuberculosis* H37Rv are shown in [Figure 3C](#). The log<sub>10</sub> CFU per spleen and lung of mice treated with the above compound/drugs after intravenous infection with  $5 \times 10^6$  CFU of *M. tuberculosis* H37Rv is shown in [Figure 3D](#).

After inoculation with  $5 \times 10^6$  CFUs of *M. tuberculosis* H37Rv per mice, all the mice in the untreated group died within 25 days after infection, whereas all of the INH (182 μmol/kg) treated mice survived till day 30. At day 30, the percent survival rates of mice treated with EMB (490 μmol/kg), compound **9d** (173 μmol/kg) and compound **9d** (87 μmol/kg) were 90%, 60%, and 40% respectively ([Fig. 3C](#)). The compound **9d** showed 2.12 log<sub>10</sub> reduction in CFU at 173 μmol/kg and approximately 1 log<sub>10</sub> reduction in CFU at 87 μmol/kg both in the lungs as well as in spleen compared to the growth in the untreated control group of mice infected with *M. tuberculosis* H37Rv ([Fig. 3D](#)). Although the in vivo efficacy of the lead compound **9d** is not better than the positive control drug INH, however, it is at least double of the EMB. Importantly, this lead compound act through a novel mechanism of action that reflects this compound as candidate molecule for further biological investigation.

## 4. Discussions

Despite the availability of highly efficacious treatment(s) for decades, TB is still a major global health problem mainly due to the emergence of MDR-, XDR- and TDR-TBs, latent/dormant

infection of TB and its synergy with HIV/AIDS. The mycobacterial  $F_0F_1$ -ATP synthase is a well validated target for TB after the success launch of bedaquiline (Sirturo™, TMC207) into the market as an effective drug for MDR-TB. Bedaquiline has shown positive efficacy against both the resistant (MDR and XDR) and latent/dormant TB strains. However, this drug has been associated with some adverse events like nausea, joint and chest pain, and headache. In addition, bedaquiline is a weak hERG blocker leading to the prolongation of the QT interval of the heart. Despite of these side effects, it is still recommended by the US-FDA specifically for the treatment of MDR-TB. Notably, there is a wide scope for further exploitation of the medicinal chemistry tools in order to identify new chemical entities targeting this validated anti-TB target that could provide new potential treatments of the MDR-, XDR- as well as TDR-TB cases. The pharmacophoric insights from the structure of bedaquiline (TMC207) have encouraged medicinal chemists to apply state-of-the-art medicinal chemistry approaches to identify and explore new chemical entities (NCEs) as potent and selective mycobacterial ATP synthase inhibitor(s).

In an effort to identify novel potent and selective mycobacterial ATP synthase inhibitors, a total of 18 new compounds designed through the state-of-the-art medicinal chemistry approaches have been synthesized and evaluated against *M. smegmatis* ATP synthase (Table 1). The observed inhibitory activity ( $IC_{50}$ ) ranges from 0.36 to 5.45  $\mu$ M. The better inhibitory activity of the sulfonamide derivatives (**9a–q**) than the precursor non-sulfonamide **8** suggests the particular importance of aromatic sulfonamide group in this class of compounds. This further substantiates the importance of structure-based drug design approach as this approach forecasted the particular importance of arylsulfonamide group for better binding and inhibition of mycobacterial ATP synthase (Fig. 2). In addition, the observed improvement in the ATP synthase inhibitory activity of the compounds (**9a–p**) possessing arylsulfonyl group than the compound **9q** possessing alkylsulfonyl group signifies the better suitability of the aromatic sulfonyl groups for potential inhibition of mycobacterial ATP synthase (Table 1).

The in vitro cell-based screening of a total of eight compounds (ATPase  $IC_{50} \leq 1 \mu$ M) against whole replicating *M. tuberculosis* H37Rv strain revealed two lead compounds (**9d** and **9e**) with MIC value of 3.12  $\mu$ g/mL (Table 2). Interestingly, these compounds lacked any cytotoxicity in both in vitro and in vivo assays conducted using Vero monkey cells and bone marrow macrophages, respectively. Notably, these two compounds did not show any cytotoxicity in vitro up to 300  $\mu$ g/mL ( $CC_{50} > 300 \mu$ g/mL), and the selectivity index for one of the compound **9d** is the highest ( $>98$ ) (Table 2). Moreover, these inhibitors caused a greater fall in cellular ATP levels than by INH or RIF which act by different mechanisms (Fig. 3A). Since these compounds seem to reduce ATP levels, the bactericidal activity of these compounds were tested on non-replicating *M. tuberculosis* H37Rv in hypoxic culture. As summarized in Table 3, the compound **9d** and **9e** caused approximately 2.4 and 1.6  $\log_{10}$  reduction in CFUs, respectively at 32-fold of their respective MICs as compared to control drug INH causing only 0.2  $\log_{10}$  reduction in CFU even at 50-fold of its MIC value. In this model, the negative control drug MTZ showed approximately 1  $\log_{10}$  reduction in CFU at 50  $\mu$ g/mL concentration.

Since ATP synthase is a universal enzyme, determining the selectivity of compounds for the mycobacterial over mammalian ATP synthase is a highly important task. For this, we used mouse liver mitochondria as the source of the mammalian ATP synthase. As summarized in Table 3, lead compounds **9d** and **9e** showed a very low inhibition (between 5 and 15%) at 100  $\mu$ M, while the positive control DCCD showed 83% inhibition of the mammalian ATP synthase. Therefore, these two lead compounds **9d** and **9e** are about 200-fold selective towards mycobacterial ATP synthase (mammalian ATPase  $IC_{50} > 100 \mu$ M). Furthermore, these lead

compounds have not shown any antibacterial or antifungal activity up to 50  $\mu$ g/mL.

The pharmacokinetic studies conducted on the compound **9d** after p.o. and IV administration in young and healthy male Sprague–Dawley rats weighing  $250 \pm 25$  g indicated its quick absorption, distribution and slow elimination. It exhibited a high volume of distribution ( $V_{ss}$ , 0.41 L/kg), moderate clearance (0.06 L/h/kg), long half life (4.2 h) and low absolute bioavailability (1.72%). The observed maximum plasma concentration ( $C_{max}$ ) and the time taken to reach the maximum plasma concentration ( $t_{max}$ ) after oral administration of this compound suggested that the compound is mainly absorbed from the stomach. Furthermore, the low clearance (0.06 L/h/kg) of this compound suggests its long acting profile (6.69 h based on  $MRT_{p.o.}$ ) (Table 4 and Fig. 3B).

In the murine model of the chronic TB, the lead compound **9d** has shown 2.12  $\log_{10}$  reductions in CFU at 173  $\mu$ mol/kg dose in both the lung and spleen of mice in comparison to the untreated control group (Fig. 3C and D). The in vivo efficacy of **9d** is at least double of EMB, thus reflecting its effectiveness towards protection against *M. tuberculosis* H37Rv. Altogether, the above detailed investigation forecasts suitability of **9d** as candidate drug for further preclinical evaluation against both replicating and non-replicating TB. This could lead to the new potential treatment of the resistant TB cases.

## 5. Conclusion

Despite the availability of highly efficacious treatment(s) for decades, TB is still a major global health problem mainly due to the emergence of MDR-, XDR- and TDR-TBs, latent/ dormant infection of TB and its synergy with HIV/AIDS. The mycobacterial  $F_0F_1$ -ATP synthase is an anti-TB target for the bedaquiline (Sirturo™), a drug recently approved by the US-FDA specifically for the treatment of MDR-TB. In our efforts to identify novel compounds as ATP synthase inhibitors, a total of eighteen new compounds designed through the state-of-the-art drug design approaches has been synthesized and evaluated against *M. smegmatis* ATP synthase where the observed inhibitory activity ( $IC_{50}$ ) ranges from 0.36 to 5.45  $\mu$ M. The in vitro cell-based screening of eight compounds (ATPase  $IC_{50} \leq 1 \mu$ M) against whole *M. tuberculosis* H37Rv has revealed four compounds (**9a**, **9c–e**) with MIC value  $\leq 6.25 \mu$ g/mL. Among these, the three compounds (**9a**, **9d** and **9e**) lacked cytotoxicity ( $CC_{50} > 300 \mu$ g/mL) in the three different cytotoxicity assay systems. The selectivity index for the compound **9d** is the highest ( $>98$ ) and has shown  $\sim 2.12 \log_{10}$  reductions in CFU both in the lungs as well as in spleen at the dose of 173  $\mu$ mol/kg as compared to the growth in the untreated control group in the murine model system. The in vivo efficacy of this compound is at least double of the ethambutol, thus suggesting this compound to be better in protection against *M. tuberculosis* H37Rv. In addition, this compound **9d** has exhibited high selectivity ( $>200$ ) towards mycobacterium than mammalian ATP synthase and good bactericidal effect ( $>2.3 \log_{10}$  reductions in CFU) in the hypoxic culture of *M. tuberculosis* at 100  $\mu$ g/mL (32 fold of its MIC) as compared to INH [ $\sim 0.2 \log_{10}$  reduction in CFU at 5  $\mu$ g/mL (100 fold of its MIC)]. The pharmacokinetics of **9d** after p.o. and IV administration in rats has indicated its quick absorption, distribution and slow elimination. It has exhibited a high volume of distribution ( $V_{ss}$ , 0.41 L/kg), moderate clearance (0.06 L/h/kg), long half-life (4.2 h) and low absolute bioavailability (1.72%). Therefore, this lead compound **9d** may be suitable as the candidate drug for further preclinical evaluation against TB.

## Acknowledgments

The authors (S.S. and K.K.R.) are thankful to Ministry of Health (MOH) and Council of Scientific and Industrial Research (CSIR),

New Delhi, respectively for financial assistance in terms of fellowship. The authors thank Dr. P. K. Shukla and Ms. Pratiksha Singh of Fermentation Technology Division, CDRI for screening lead compounds against bacteria and fungi. The Sophisticated Analytical Instrument Facility (SAIF) department is acknowledged for the characterization of compounds. The technical assistances of Messrs A. S. Kushwaha, D. N. Vishwakarma and Zahid Ali are also acknowledged.

### Supplementary data

Supplementary data associated with this article can be found, in the online version, at <http://dx.doi.org/10.1016/j.bmc.2014.12.060>.

### References and notes

- World Health Organization. Global Tuberculosis Report. WHO Report 2013; WHO Press: Geneva, Switzerland, 2013.
- Koul, A.; Arnoult, E.; Lounis, N.; Guillemont, J.; Andries, K. *Nature* **2011**, 469, 483.
- Migliori, G. B.; Centis, R.; D'Ambrosio, L.; Spanevello, A.; Borroni, E.; Cirillo, D. M.; Sotgiu, G. *Clin. Infect. Dis.* **2012**, 54, 1379.
- Udwadia, Z. F. *Thorax* **2012**, 67, 286.
- Udwadia, Z. F.; Amale, R. A.; Ajbani, K. K.; Rodrigues, C. *Clin. Infect. Dis.* **2012**, 54, 579.
- Mitchison, D. A. *Am. J. Respir. Crit. Care Med.* **2005**, 171, 699.
- Vandiviere, H. M.; Loring, W. E.; Melvin, I.; Willis, S. *Am. J. Med. Sci.* **1956**, 232, 30. *passim*.
- Wayne, L. G.; Hayes, L. G. *Infect. Immun.* **1996**, 64, 2062.
- Andries, K.; Verhasselt, P.; Guillemont, J.; Gohlmann, H. W.; Neefs, J. M.; Winkler, H.; Van Gestel, J.; Timmerman, P.; Zhu, M.; Lee, E.; Williams, P.; de Chaffoy, D.; Huitric, E.; Hoffner, S.; Cambau, E.; Truffot-Pernot, C.; Lounis, N.; Jarlier, V. *Science* **2005**, 307, 223.
- Koul, A.; Dendouga, N.; Vergauwen, K.; Molenberghs, B.; Vranckx, L.; Willebrords, R.; Ristic, Z.; Lill, H.; Dorange, I.; Guillemont, J.; Bald, D.; Andries, K. *Nat. Chem. Biol.* **2007**, 3, 323.
- Matteelli, A.; Carvalho, A. C.; Dooley, K. E.; Kritski, A. *Future Microbiol.* **2010**, 5, 849.
- Khan, S. R.; Singh, S.; Roy, K. K.; Akhtar, M. S.; Saxena, A. K.; Krishnan, M. Y. *Int. J. Antimicrob. Agents* **2013**, 41, 41.
- World Health Organization. The Use of Bedaquiline in the Treatment of Multidrug-resistant Tuberculosis. Interim Policy Guidance (WHO/HTM/TB/2013.6). Geneva, Switzerland, November 2013.
- Anti-Infective Drugs Advisory Committee Meeting Report. The U.S. Food and Drug Administration., November 28, 2012.
- Haagsma, A. C.; Podasca, I.; Koul, A.; Andries, K.; Guillemont, J.; Lill, H.; Bald, D. *PLoS ONE* **2011**, 6, e23575.
- de Jonge, M. R.; Koymans, L. H.; Guillemont, J. E.; Koul, A.; Andries, K. *Proteins* **2007**, 67, 971.
- Rastogi, V. K.; Girvin, M. E. *Nature* **1999**, 402, 263.
- Singh, S.; Roy, K. K.; Khan, S. R.; Kashyap, V. K.; Sharma, S. K.; Krishnan, M. Y.; Chaturvedi, V.; Sinha, S.; Srivastava, R.; Saxena, A. K. WO2013102936 (A4), September 12, 2013.
- McClatchy, J. K. *Lab. Med.* **1978**, 9, 47.
- Lenaerts, A. J.; Gruppo, V.; Marietta, K. S.; Johnson, C. M.; Driscoll, D. K.; Tompkins, N. M.; Rose, J. D.; Reynolds, R. C.; Orme, I. M. *Antimicrob. Agents Chemother.* **2005**, 49, 2294.
- Frezza, C.; Cipolat, S.; Scorrano, L. *Nat. Protoc.* **2007**, 2, 287.
- Garcia, J. J.; Ogilvie, I.; Robinson, B. H.; Capaldi, R. A. *J. Biol. Chem.* **2000**, 275, 11075.
- Anoopkumar-Dukie, S.; Carey, J. B.; Conere, T.; O'Sullivan, E.; van Pelt, F. N.; Allshire, A. Br. J. Radiol. **2005**, 78, 945–947.
- Mosmann, T. J. *Immunol. Methods* **1983**, 65, 55.
- Kelly, B. P.; Furney, S. K.; Jessen, M. T.; Orme, I. M. *Antimicrob. Agents Chemother.* **1996**, 40, 2809.
- Dmitriev, O. Y.; Abildgaard, F.; Markley, J. L.; Fillingame, R. H. *Biochemistry* **2002**, 41, 5537.